

Toward a comprehensive understanding of solid-state core-level XPS linewidths: Experimental and theoretical studies on the Si 2*p* and O 1*s* linewidths in silicates

G. M. Bancroft,^{1,*} H. W. Nesbitt,² R. Ho,² D. M. Shaw,³ J. S. Tse,³ and M. C. Biesinger⁴

¹*Department of Chemistry, University of Western Ontario, London, Ontario, Canada N6A 5B7*

²*Department of Earth Sciences, University of Western Ontario, London, Ontario, Canada N6A 5B7*

³*Department of Physics, University of Saskatchewan, Saskatoon, Saskatchewan, Canada S7N 5E2*

⁴*Surface Science Western, University of Western Ontario, London, Ontario, Canada N6A 5B7*

(Received 28 April 2009; published 4 August 2009)

High resolution X-ray Photoelectron Spectroscopy (XPS) core-level Si 2*p* and O 1*s* spectra of the nonconductors α -SiO₂ (quartz) at 120 and 300 K and vitreous SiO₂ at 300 K were obtained with a Kratos Axis Ultra XPS instrument (instrumental resolution of <0.4 eV) which incorporates a unique charge compensation system that minimizes differential charge broadening on nonconductors. The Si 2*p* and O 1*s* linewidths at 300 K (\sim 1.1 and \sim 1.2 eV, respectively) are similar for all silicates (and similar to previous thin film SiO₂ spectra obtained previously), showing that differential charging does not contribute significantly to our spectra. At 120 K, there is a small decrease (0.04 eV) in the Si 2*p* linewidth of α -SiO₂, but no measurable decrease in O 1*s* linewidth. The O 1*s* lines are generally and distinctly asymmetric. We consider all possible sources of line broadening and show that final state vibrational broadening (FSVB) and phonon broadening are the major causes of the broad and asymmetric lines. Previous high resolution gas phase XPS studies have identified large FSVB contributions to the Si 2*p* spectra of SiCl₄, SiF₄, and Si(OCH₃)₄ molecules, and this vibrational structure leads total Si 2*p*_{3/2} linewidths of up to \sim 0.5 eV, even with individual peak linewidths of <0.1 eV. The Si atom of Si(OCH₃)₄ is an excellent analog for Si in crystalline SiO₂ because the Si-O bond lengths and symmetric stretch frequencies are similar in both compounds. Similar vibrational contributions to the Si 2*p* and O 1*s* spectra of solid silicates are anticipated if the Si 2*p* and O 1*s* core-hole states produce similar changes to the Si-O bond length in both phases. To investigate the possibility, Car-Parrinello molecular dynamics calculations were performed and show that changes to Si-O bond lengths between ion and ground states (Δr) for both Si 2*p* and O 1*s* hole states are similar for both crystalline SiO₂ and gaseous Si(OCH₃)₄. Δr are -0.04 Å for Si 2*p* and $\sim+0.05$ Å for O 1*s* in both compounds. Indeed, the vibrational envelope from the Si 2*p* spectrum of Si(OCH₃)₄, broadened to our instrumental linewidth of 0.4 eV, accounts for the majority (\sim 0.8 eV) of the Si 2*p*_{3/2} linewidth for crystalline SiO₂ (\sim 1.1 eV) with phonon broadening accounting for the remainder. The results provide excellent support for the tenet that final state vibrational splitting, as seen in the gas phase molecules, similarly affects the solid-state spectra. The calculations also indicate that the O 1*s* linewidths should be larger than the Si 2*p* linewidths, as observed in our spectra. FSVB should also lead to small peak asymmetries, as seen in the O 1*s* spectra. The contribution of phonon broadening to the linewidth is also evaluated and shown to be comparable to the FSVB contribution at 120 and 300 K but considerably smaller at very low temperatures.

DOI: 10.1103/PhysRevB.80.075405

PACS number(s): 79.60.Bm, 71.15.Mb

I. INTRODUCTION

O 1*s* X-ray Photoelectron Spectroscopy (XPS) spectra and core-level spectra of many other elements in oxides are widely used to obtain chemical state information of oxygen and metal species in and on solids and surfaces before and after chemical reactions. With the advent of high resolution synchrotron x-ray sources, high resolution electron analyzers, and effective charge neutralization systems (e.g., Kratos Axis Ultra instrument) which dramatically decrease charge broadening for “rough” nonconductor surfaces, experimental core-level spectra are now highly reproducible for nearly all types of solid surfaces. Core-level XPS spectra and particularly O 1*s* spectra consequently have been used ever more widely to characterize bulk and thin film simple oxides (e.g., see very recent references to pristine, thin films, modified thin films, or reacted surfaces such as TiO₂,^{1–7} SiO₂ and silicates,^{8–13} RuO₂,^{14,15} MgO,^{16–18} CaO,¹⁹ ZnO,²⁰ Fe₃O₄,²¹ Cu₂O,²² and other transition metal oxides;^{23–25} also see a recent review of ambient pressure XPS on oxides²⁶).

Recent XPS studies on nonconductor glasses,^{27–30} complex superconductor oxides,^{31–33} ceramics,^{34,35} and surface reactions of many oxygen-containing molecules on a wide variety of substances^{36–39} have also reported narrower O 1*s* and other core-level linewidths than previously collected. Because the majority of these substrates are nonconductors, many recent studies have been conducted using the Kratos instrument with its novel magnetic confinement charge compensation system. The instrument has yielded reproducible O 1*s* and other core-level spectral line shapes and linewidths on both atomically smooth and rough nonconductor surfaces: the O 1*s* linewidths, for example, are often much narrower^{8–11,27–29} than previously obtained with other instruments for bulk nonconductors. Moreover, nonconductor linewidths have been shown to be just as narrow as obtained for semiconductors⁸ or metals.⁴⁰ For example,⁴⁰ VO₂ exhibits an insulator-metal transition above 300 K and the O 1*s* linewidth at 270 K of the insulator phase of VO₂ (measured from Fig. 3 of Ref. 40 as 1.0 eV) is as narrow as (or slightly narrower than) the linewidth of the metallic phase at 320 K

(measured as at least 1.1 eV). O 1s linewidths for the metallic phase are difficult for us to simply measure off a published figure because of the Doniach-Sunjić asymmetry, which was not quantified in Ref. 40.

Although surface charging has been largely overcome with technical advances, core-level linewidths of oxides remain surprisingly large. In most of the above studies, the O 1s and other core-level spectra were fitted with symmetric Gaussian/Lorentzian or Voigt line shapes and fits yielded O 1s linewidths commonly greater than 1.0 eV [e.g., about 1.2 eV for silicates^{8–11,27–29} and about 1.4 eV for MgO (Refs. 16–18)]. The O 1s linewidths on the semiconductor TiO₂ and other transition metal oxides and superconductors are narrower, but still usually ≥ 1.0 eV, except for Cu₂O,²² RuO₂,^{14,15} and the superconductors Sr₂CuO₂Cl₂ and Ca₂CuO₂Cl₂.³³ The O 1s linewidths on the bulk semiconductor Cu₂O (Ref. 22) at room temperature appear to be the narrowest O 1s linewidth yet published at 0.7 eV; while for metallic RuO₂ films^{14,15} the O 1s linewidths at 100 K were ~ 0.75 eV (both results obtained with high resolution synchrotron radiation sources with a total experimental resolution of less than 0.2 eV). It is also apparent from Si 2p_{3/2} spectra of silicates, Ti 2p_{3/2} spectra for TiO₂, and Ru 3d_{5/2} spectra of RuO₂ that the metal linewidths are usually narrower than the O 1s linewidths for a given compound. Indeed, the Ru 3d_{3/2} linewidth of the conducting RuO₂ films on Ru metal is ~ 0.5 eV, whereas the O 1s linewidth is ~ 0.75 eV.

In addition to broad lines, some O 1s spectra (e.g., MgO, CaO, and silicates) display a small but distinct asymmetry making it necessary to fit an additional peak (10–20 % of the intensity of the main peak) usually on the high binding energy side of the peak.^{13,28} The high energy peak has sometimes been assigned to an “additional” chemical species.^{13,28,35,39}

Questions arise from the above results: (1) why are these O 1s linewidths so broad and variable (0.7 to >1.3 eV) relative to observed individual linewidths of 50–150 meV for Si 2p, C 1s, P 2p, and B 1s spectra of polyatomic molecules in the gas phase;^{41–45} (2) why are they much broader than total linewidths observed for semiconductor solids such as Si,^{46–48} PbS (Ref. 49) (<0.3 eV), FeAsS and FeS₂ (Ref. 50) (<0.5 eV), and for other nonconductors such as As₂S₃ (Ref. 8) (~ 0.5 eV); (3) should the O 1s line shapes be symmetric when there is only one structural O species in an oxide; and (4) why are the metal linewidths generally narrower than the O 1s linewidths for a given oxide?

Traditionally, large solid-state linewidths have been attributed to phonon broadening (PB). In 1974, Citrin *et al.*⁵¹ published temperature dependent monochromatic XPS spectra of the potassium and halide core levels on thin film potassium halides. The measured linewidths of about 1 eV were corrected for the instrumental effects (photon and electron linewidths). The temperature dependence of the nonconductor linewidths (better seen in the core-level metal spectra⁵¹) was shown to be consistent^{51–53} with phonon broadening from excitation of a large number of phonons produced in response to hole production. Phonon broadening should lead to symmetric Gaussian^{51–53} line shapes, and there was no evidence for asymmetry in the experimental spectra of the alkali

halides. The phonon contribution explained the temperature dependence of the linewidths, but the corrected experimental linewidths were, at all temperatures, larger than calculated,⁵¹ with no explanation provided. Furthermore, separate calculations yielded large differences (>0.2 eV) in the calculated linewidths.^{51–53} Finally, the linewidths extrapolated to 0 K [here referred to as $\Gamma_{\text{PH}}(0)$] have large uncertainties because extrapolations of experimental data extended over an ~ 300 °C range.

The extrapolations, nevertheless, indicate $\Gamma_{\text{PH}}(0)$ values much greater than inherent linewidths expected from final state lifetime contributions.

Another possible major contribution to solid-state line broadening is “final state” vibrational splitting and broadening which arise from the difference in bond lengths between the ground state and ion state. Siegbahn *et al.*⁵⁴ first showed that final state vibrational broadening (FSVB) contributed to the C 1s spectrum of CH₄ gas. Bancroft and co-workers^{41,55} later demonstrated the importance of this vibrational splitting on polyatomic gas phase Si compounds. Unlike PB, FSVB is *temperature independent* and can lead to asymmetric line profiles. In the last 10 years Thomas *et al.*⁴² obtained optimized spectra on the C 1s spectra of a host of gas phase C compounds as well as the Si 2p, P 2p, and B 1s spectra on Si, P, and B compounds.^{43–45} The vibrationally resolved O 1s spectrum of gas phase H₂O has also been reported, yielding an inherent O 1s linewidth of 160 meV.⁵⁶ These results demonstrated the following: (1) lifetime contributions to the overall band profile are small (e.g., in SiF₄, the inherent individual peak width is 79 meV compared to the overall Si 2p_{3/2} profile width of ~ 0.5 eV); (2) FSVB is the controlling factor on the overall linewidth; (3) the symmetric *M-X* stretching frequency dominates most spectra, although for the O 1s spectrum of H₂O the bending mode is dominant;⁵⁶ (4) the total linewidth for a vibrational profile increases linearly with the symmetric stretch frequency [see Si 2p spectra of SiCl₄ and SiF₄ (Ref. 43)]; and (5) vibrational profiles are invariably asymmetric to higher binding energies.

For adsorbed molecules on surfaces, Martensson and Nilson⁵⁷ suggested that FSVB contributes to the overall widths of core-level spectra of adsorbed species (e.g., C 1s and O 1s of CO). Andersen *et al.*⁵⁸ and Folisch *et al.*,⁵⁹ using high resolution synchrotron radiation, then resolved and characterized the C-H and C-O final state vibrational splittings (from the symmetric stretch) on the C 1s peaks of adsorbed ethylenes and CO, respectively. The resolved C 1s peaks were broadened somewhat relative to the gas phase spectra of C₂H₄ and CO because of low-energy “cooperative” vibrational modes, analogous to the phonon broadening in bulk solids. A large number of papers have reported both types of splitting and broadening to the core-level spectra of adsorbed species (for a recent paper see Ref. 60). Also, recently, Bergersen *et al.*⁶¹ observed both types of vibrational splitting and broadening in the C 1s spectra of CH₄ clusters of up to 1000 molecules.

To our knowledge, there has been only one mention in the literature of the importance of FSVB on the core-level XPS spectra of bulk solids. It was suggested⁸ that this final state vibrational splitting dominates the Si 2p linewidth in solid-state silicates such as Mg₂SiO₄, just as it dominates the over-

all Si $2p$ linewidth in the gas phase analog $\text{Si}(\text{OCH}_3)_4$.⁵⁵ However, Andersen *et al.*⁶² reported resolved asymmetric vibrational structure (vibrational splitting of 58 meV) on the high resolution Be $1s$ XPS spectrum of Be metal. They attributed this structure to a resolved phonon effect. Because of the large calculated difference in Be-Be bond length between ground and ion state,⁶³ it appears to us that the resolved vibrational profile in the Be $1s$ XPS of Be metal is more likely due to final state vibrational splitting. Coincidentally, the calculated Be $1s$ profile in molecular Be_2 is very similar to that of Be metal.⁶⁴

It is important to show that both phonon broadening and final state vibrational contributions are the important contributors to the broad core-level spectra of solids (as for the above adsorbates and clusters) for at least two very practical reasons. First, it may be possible to obtain much narrower O $1s$ (and other core-level) linewidths on nonconductors in the future by cooling samples to low T and using synchrotron radiation to obtain the highest experimental resolution and second, many O $1s$ and other core-level spectra may be inherently asymmetric as expected when final state vibrational splitting is a dominant contribution to these core-level spectra. Recognition of asymmetry is especially important, otherwise small deviations from symmetric O $1s$ peaks may be interpreted as small additional peaks from moieties with unique chemical shifts.

In this paper, we present experimental and theoretical evidence for the importance of FSVB on the Si $2p$ and O $1s$ XPS spectra of silicates. High-level MD calculations are critical to show that the final state vibrational effects in a silicate should be very similar to those already observed on gas phase silicon analogs and that the broadening (and asymmetry) of the O $1s$ spectra should, if anything, be larger than for the Si $2p$ spectra. After addressing possible causes of line broadening (e.g., inherent linewidth differences, differential charging, inhomogeneous work functions, and surface chemical shifts), we show that the observed Si $2p$ and O $1s$ linewidths in silicates can be understood using the combination of FSVB and PB.

II. EXPERIMENTAL METHODS

A gem-quality α -quartz (SiO_2) specimen (the same as used previously⁸) was obtained from the UWO Dana collection, and pure vitreous SiO_2 was obtained commercially. Their purity was characterized by broad scan XPS spectra that showed no impurities other than the usual small C $1s$ peak from ubiquitous carbon. Both samples were fractured *in situ* in the vacuum of the transfer chamber (low 10^{-8} Torr range) and immediately transferred to the analytical chamber where pressures were in the low 10^{-9} Torr range. Quartz has no cleavage so that its fracture exposes an irregular surface. Fracture of vitreous silica produces a conchoidal fracture surfaces. For the most general use of the XPS technique, it is important to be able to get the “minimal” linewidths on rough surfaces of nonconductors.

A Kratos Axis Ultra x-ray photoelectron spectrometer (with magnetic confinement charge compensation system)⁶⁵ at Surface Science Western was used to collect the XPS

spectra using Al $K\alpha$ radiation at 1486.71 eV and a $300 \times 700 \mu\text{m}^2$ spot size for all analyses. A sea of nondirectional low-energy electrons above the sample are trapped by a magnetic field and are available to compensate for different chargings on a sample surface. The take-off angle was 90° . Spectra were run at room temperature (295 K), but the sample surfaces heated up to about 300 K in the x-ray beam. The SiO_2 was run at 120 K as well (100 K backing plate temperature) to observe the change in Si $2p$ and O $1s$ linewidths with temperature. A 10 eV pass energy was used to collect all core levels (Si $2p$, S $2p$, C $1s$, Ti $2p$, and O $1s$). The instrumental resolution at 10 eV pass energy is <0.4 eV.^{8–11} The very small C $1s$ signal on all spectra indicated minimal C contamination. The charge compensation system was tested for effectiveness over a large range of settings with only very small changes (<0.03 eV) in linewidths. These widths were highly reproducible for all minerals over months of testing on different fractured samples. However, our experience with this instrument over several years has resulted in a slight improvement in linewidths—for example, we reported overall Si $2p$ linewidths of 1.36 eV for forsteritic olivine (Mg_2SiO_4) in 2004 (Ref. 8) and 1.26 eV in 2008.⁹ However, the Si $2p$ and O $1s$ linewidths for SiO_2 at 300 K are identical to those reported 3 years ago⁹ (Table I). The linewidth can be slightly sensitive (less than 0.03 eV increase) if the surface carbon contamination is large or if the charge neutralizer plates become highly contaminated.

Core-level spectra were fitted with a 70% Gaussian–30% Lorentzian function as in previous papers.^{8–11} Slightly different functions (e.g., 50% Gaussian) sometimes gave slightly better fits with very small changes (<0.05 eV) in linewidth. Spin-orbit components were constrained to have the same linewidths. The Si $2p$ spin-orbit splitting was fixed to atomic values [0.617 eV (Ref. 56)], and the $p_{1/2}$ peak was constrained to half the intensity of the $p_{3/2}$ peak. Because of the constraints on the $p_{1/2}$ position, linewidth, and intensity, just the $p_{3/2}$ position and linewidth were iterated to minimize the root mean square deviations for a given spectrum. All spectra were corrected for the background using the Shirley approach.⁶⁶ CASAXPS software⁶⁷ was used to fit all the spectra.

Thomas *et al.*⁴³ kindly provided the raw data for their optimized high resolution gas phase spectra of SiF_4 and SiCl_4 , for which the instrumental resolution was 30 meV and the inherent lifetime Si $2p$ widths were 79 and 54 meV respectively. The total observed individual linewidths of about 87 and 57 meV, respectively, made it possible to resolve completely a rich vibrational structure involving nine vibrational peaks separated by the symmetric stretching frequency in the ion state (about 10% larger than the measured ground state vibrational frequency). Our previous medium resolution Si $2p$ spectrum (instrumental resolution of 0.15 eV) of $\text{Si}(\text{OCH}_3)_4$ (a better analog to SiO_2) showed a very similar vibrational envelope (ten peaks) to the above optimal spectra for SiF_4 and SiCl_4 .⁵⁵ To simulate the lower resolution Si $2p$ solid-state spectra (e.g., at our resolution of 0.4 eV) we used the raw spectra of SiF_4 , SiCl_4 , and $\text{Si}(\text{OCH}_3)_4$ and broadened the individual peak linewidths to a maximum value of 0.8 eV. The resulting broadened Si $2p$ spectra were then fit to a Si $2p$ doublet and the Si $2p_{3/2}$ linewidth obtained.

III. COMPUTATIONAL METHODS

A. Structural models

Car-Parrinello molecular dynamics (CPMD)⁶⁸ within the density functional theory formalism was used to obtain changes in Si-O bond lengths in solid-state SiO₂ (α quartz) and gas phase Si(OCH₃)₄ resulting from core ionization of Si (removal of a Si 2*p* or Si 1*s* electron) and O (removal of an O 1*s* electron). The Perdew-Burke-Enzerhof (PBE) exchange correlation functional⁶⁹ was employed in the calculations. The core electrons were treated using a Troullier-Martins norm-conserving pseudopotential approach.⁷⁰ Pseudopotentials for the ground state and partially screened O 1*s* and Si 1*s* and 2*p* cores were employed to investigate the effect of partial screening on the structure and dynamics of α quartz. The ground state Si and O pseudopotentials were taken from the CPMD pseudopotential library. Previous work on silicate minerals has shown that these pseudopotentials yield satisfactory results for silicate compounds.^{71,72} Pseudopotentials for the (partially screened) half-core-hole (HCH) calculations were generated by removing half an electron from the relevant core levels. This half-core approximation, which originates from Slater's transition state theory,⁷³ is normally used to calculate core-level spectra such as the x-ray absorption near edge structure in SiO₂ polymorphs,⁷⁴ and in principle the relaxation energy is correct to second order via perturbation theory. A calculation was also performed after removing a full-core electron for comparison. Valence electrons were modeled using a plane wave basis with an energy cutoff of 90 Ry. Energy sampling was done for the Γ point only. As a test of the pseudopotentials for the ground state, the geometry of the initial quartz structure was optimized using the preconditioned conjugate gradient approach where convergence was achieved when the largest forces on the nuclei dropped below 0.0001 hartree/bohr.

The initial structure for α quartz was generated from known crystal coordinates obtained from the American Mineralogist crystal structure database.⁷⁵ The unit cell had four SiO₂ units in a hexagonal cell with cell parameters $a = 4.914$ Å and $c = 5.406$ Å in the *P3121* space group.⁷⁶ This cell was then transformed to the orthorhombic space group, yielding cell parameters of $a = 4.914$ Å, $b = 8.511$ Å, and $c = 5.406$ Å. A (2×1×2) supercell with 24 SiO₂ units was then generated. Previous work on hydrous olivine⁷¹ and forsterite⁷² has shown that the *k*-point sampling and supercell size on silicate compounds are expected to yield satisfactory results. Indeed, the bond lengths reported here for the ground state structure are in very good agreement with the recent crystallographic data.

As a test of the quartz calculations, a similar set of runs was done for an isolated tetramethoxysilane molecule, Si(OCH₃)₄. This molecule gives a reasonable approximation to the SiO₄ unit in α quartz, and experimental data on the structure and vibrational dynamics⁷⁷ are available. The Si(OCH₃)₄ input geometry was generated with Molden,⁷⁸ and the geometry was optimized using the PBE functional and a 6-311++g** Pople basis set within the rational function optimization approach in GAUSSIAN03.⁷⁹ The convergence was reached when the largest force on the atoms was less than 0.000 45 hartree/bohr. An analysis of the harmonic frequencies indicated that a minimum had been reached. A check of the structure with the experimental geometry reported in Ref. 74 indicated the structure was a good starting geometry to the CPMD calculations.

B. Molecular dynamics

The electronic ground states, and partially screened states, for SiO₂ and Si(OCH₃)₄ were first quenched to the Born-Oppenheimer surface. Molecular dynamics simulations were

TABLE I. Si 2*p*_{3/2} and O 1*s* XPS linewidths (FWHM), Si-O symmetric stretching frequencies, and Debye Temperatures for solid silicates along with Si 2*p*_{3/2} linewidths for gaseous SiF₄, SiCl₄, and Si(OCH₃)₄.

Compound	<i>T</i> (K)	ΔE (eV) ^a	Si 2 <i>p</i> _{3/2} FWHM (eV)	O 1 <i>s</i> FWHM (eV)	Si-O stretch (cm ⁻¹)	Θ_D (K)
α -SiO ₂ ^b	120	0.4	1.09(0.01)	1.23(0.01)	1081 ^{c,d}	528 ^e ,562 ^f
	300	0.4	1.13(0.01)	1.23(0.01)		
SiO ₂ glass ^b	300	0.4	1.16(0.02)	1.27(0.02)	1095 ^{e,g}	~645 ^h
SiO ₂ film ⁱ	300	0.2	1.06			
Mg ₂ SiO ₄ ^j	300	0.4	0.99(0.03)	1.24(0.03)	830 ^{c,d,k}	763 ^l ,647 ^e
SiF ₄ ^m	295	0.03	~0.46		801 ^o	
ⁿ	295	0.10	~0.5			
SiCl ₄ ^m	295	0.03	~0.25		423 ^o	
Si(OCH ₃) ₄ ^p	295	0.15	~0.6		840 ^p	

^aTotal instrumental resolution (photon plus electron) in eV.

^bThis work.

^cReference 98.

^dReference 82.

^eReference 99.

^fReference 100.

^gReference 83.

^hThis value is for the SiO₂ polymorph coesite (from Ref. 5 above) which should be a good approximation for silica glass.

ⁱReference 80.

^jAverage from Refs. 8 and 10.

^kReference 93.

^lReference 82.

^mReference 43.

ⁿReference 41.

^oReference 101.

^pReference 55.

performed at 80 and 300 K using the Car-Parrinello approach for the electron dynamics and a classical approach for the nuclei. The molecular dynamics runs were performed in the microcanonical (NVE) ensemble. Identical pseudopotentials, functional, and energy sampling were employed for molecular dynamics runs as described above. The electron mass employed was 800 a.u. and a time step of 0.12 fs was used. Thermodynamic equilibrium was achieved in 1.8 ps and essential quantities (coordinates, velocities) were computed over an additional 1.2 ps. The temperature of the system for the equilibration runs was maintained by employing a simple velocity rescaling scheme. For the data collection runs, the temperature scaling was removed, though the temperature was monitored to ensure that it did not deviate from the equilibrium value. Molecular dynamics runs were generated for the ground state, O $1s$, Si $1s$, and Si $2p$ partially screened systems.

IV. RESULTS

A. Si $2p$ and O $1s$ XPSs of quartz and vitreous SiO₂

Figure 1 illustrates the Si $2p$ and O $1s$ XPS spectra of α -SiO₂ at 300 K [Figs. 1(a) and 1(d)], α -SiO₂ at 120 K [Figs. 1(b) and 1(e)], and vitreous SiO₂ at 300 K [Figs. 1(c) and 1(f)]. Linewidths are shown (with standard deviations) in Table I for these compounds, along with previously obtained linewidths for a thin SiO₂ film on Si (Ref. 80) and for another silicate olivine (Mg₂SiO₄).⁸ The reproducibility of linewidths and peak shapes is excellent. For example, six separate spectra at 120 K and five separate spectra at 300 K for both Si $2p_{3/2}$ and O $1s$ of α -SiO₂ (one spectrum at each T is shown in Fig. 1) yielded linewidths with a total range of 0.03 eV. Also, the linewidths at 300 K are identical to those previously reported for α -SiO₂.⁹ The linewidths for the crystalline and vitreous phases of SiO₂ are within 0.07 eV, and our Si $2p_{3/2}$ linewidths on α -SiO₂ are within 0.07 eV of the Si $2p$ linewidth for a higher resolution (instrumental resolution of 0.2 eV compared to our resolution of 0.4 eV) spectrum of a thin ~ 30 Å film where charging is not a problem.⁸⁰ An earlier high resolution XPS study of similar thin SiO₂ films on Si gave a slightly larger Si $2p_{3/2}$ linewidth [1.15–1.20 eV (Refs. 8 and 48)]. Also, Si $2p$ and O $1s$ linewidths for polycrystalline SiO₂ suspensions⁸¹ and siloxane polymers containing SiO₄ moieties³⁹ yield very similar Si $2p$ and O $1s$ linewidths. These results (along with those reported in Refs. 8 and 40) provide confidence that reproducible minimal linewidths can be obtained on smooth and rough surfaces of nonconductors and even polycrystalline samples, using the Kratos charge compensation system. The results also show that the Si $2p_{3/2}$ and O $1s$ linewidths are similar in *all* compounds containing a SiO₄ unit so far studied.

In addition, the Si $2p$ spectra of Si molecules^{41,43,55} have been collected at high instrumental resolution using synchrotron radiation (Table I), so that vibrational structure is readily resolved. The total width of the Si $2p_{3/2}$ vibrational envelopes for these gases (see Sec. IV B and Fig. 4 for the details) can be greater than 0.5 eV even with an instrumental resolution of 0.03 eV.^{41,43,55}

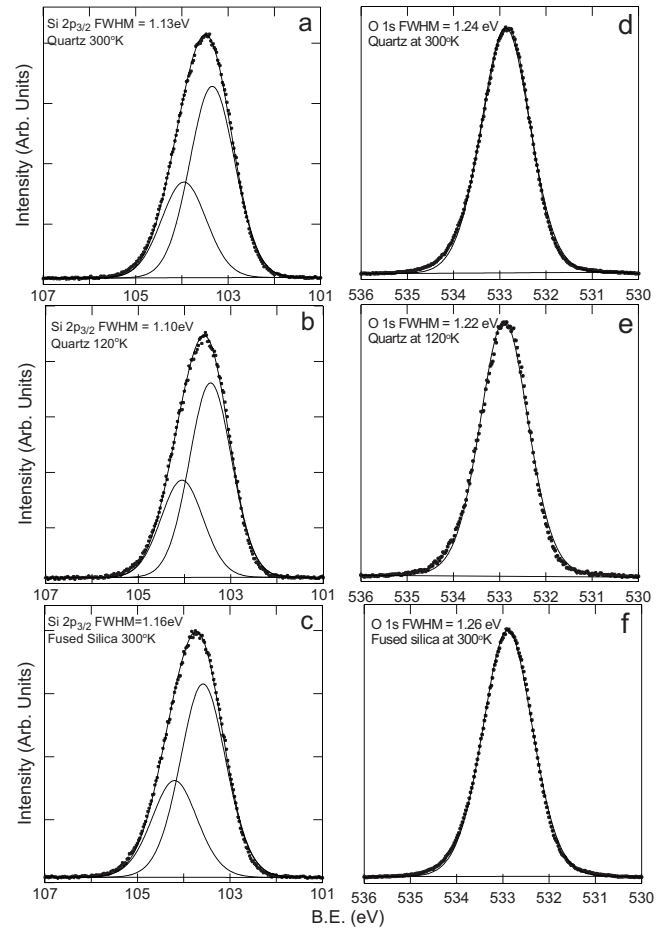


FIG. 1. High resolution Si $2p$ and O $1s$ XPS spectra: (a) and (d) α quartz at 300 K; (b) and (e) α quartz at 120 K; and (c) and (f) SiO₂ glass at 300 K.

Also reported in Table I are the symmetric Si-X ($X = O, F, Cl$) stretching frequencies along with the Debye temperatures for the bulk solids. The silicate species show quite a range of frequencies in Table I, 830 cm⁻¹ for Mg₂SiO₄ with a SiO₄ unit with no Si-O-Si bonds to 1081 cm⁻¹ for completely “condensed” SiO₂ with all Si-O-Si bonds. These differences are used to assign the degree of Si-O-Si bonding in glasses from IR or Raman spectra.^{82,83} As mentioned above, it is the symmetric stretch in the core ionized state that dominates the XPS spectra of gas phase molecules, especially for the “central” atom in symmetric species such as Si in SiX₄ ($X = H, F, Cl, OCH_3$),^{41,43,55} B in BF₃,⁴⁴ P in PF₃,⁴⁵ or C in CH₄.^{53,84} The Debye temperature is critical for the ensuing analysis of the phonon broadening.^{51–53} Note that the Debye temperature for Mg₂SiO₄ is substantially higher than that for α -SiO₂.

Three general observations are apparent from the solid-state linewidths in Table I. First, the Si $2p$ and O $1s$ linewidths and line shapes for all the three SiO₂ samples in Table I are within 0.1 eV at 300 K. In our recent studies of silicate minerals and glasses, the O $1s$ linewidths at 300 K for all samples (including minerals and glasses) are between 1.21 and 1.28 eV.^{9–11,27,28} Similarly, the O $1s$ linewidths are all very similar for TiO₂ and amorphous and crystalline SrTiO₃ and BaTiO₃.^{5,29} Second, the Si $2p_{3/2}$ widths are always about

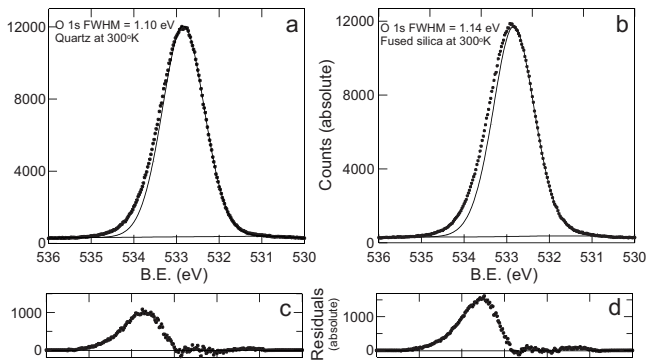


FIG. 2. One peak fits (optimized to the low binding energy part of the peak of the XPS spectra at 300 K: (a) O 1s of α quartz; (b) O 1s of silica glass. Note the residuals below the spectra which show the size of the extra peak that would be required to fit these overall spectra.

0.2 eV narrower than the O 1s linewidths. Third, there is a small increase in the Si 2p linewidth of SiO₂ with increase in T from 120 to 300 K, but the O 1s linewidth does not change noticeably over this temperature range.

The fits to the Si 2p spectra are reasonable, giving no evidence for asymmetry in the peaks; but the spin-orbit doublet fits will tend to mask any peak asymmetry. In contrast, the one-peak fits to the O 1s spectra [Figs. 1(d)–1(f)] do not provide good fits to the “wings” of the spectra. We illustrate a one-peak fit to two of the O 1s spectra at 300 K in Fig. 2. The fits were optimized to reproduce the low binding energy part of the spectrum. Although a good fit is obtained to this part of the peak, the high binding energy side of the peak is very poorly fit. A second low intensity peak is needed to fit these O 1s peaks satisfactorily (see the residuals in Fig. 2). For each fit, the second (minor) peak is about 0.9 eV above the main peak and has about 10% of the intensity of the main peak. These fits are similar to a recently published olivine and SiO₂ O 1s spectra.^{13,28,81} These spectra provide evidence that the O 1s peaks from the bulk O are *inherently* asymmetric and that all have similar asymmetry. Because of the different O 1s binding energies for the three SiO₂ compounds and for Mg₂SiO₄ (e.g., close to a 2 eV difference between the O 1s binding energies in SiO₂ and Mg₂SiO₄), the similar degree of asymmetry makes unlikely the possibility that OH[−] or H₂O species^{1,11} contribute to the O 1s asymmetry in any of these compounds. For example, the O 1s peak for OH[−] [at 532.0 eV (Ref. 11)] would be on the high binding energy side of the olivine O 1s peak at 531.0 eV (Ref. 11) but on the low binding energy side of the O 1s peak for quartz at 532.8 eV.

B. Change in bond lengths in solid and gas phases after ionization

The vibrational splitting and broadening in the *gas* phase spectra arise because of bond length changes (Δr) accompanying the core-level transition from the ground to the ion state.^{41–43,54} A Frank Condon analysis of the electronic transitions from ground state to ion state in the photoelectron process yields an XPS vibrational envelope with more vibra-

tional peaks (and broader overall peak envelope) as Δr and the magnitude of the vibrational splitting increases. In the case of Si, B, and P molecules,^{41,43–45} Δr is 0.06 Å. It is interesting to note that most recent theoretical calculations yield a Δr value closer to 0.04 Å.⁴⁴ The core equivalent model^{55,84–87} (e.g., P⁺⁵ is the core equivalent for Si⁴⁺) suggests that Δr should remain the same for a given element (e.g., Si) regardless of its bonding partner. The experimental Si 2p spectra indicate that Δr for SiH₄, SiF₄, and SiCl₄ and their core equivalents are all 0.06 Å, a value consistent with a constant value expected from the core equivalent model. The actual difference in M -O bond lengths between silicates and their core equivalent phosphates is closer to 0.09 Å (Ref. 31 in Ref. 10), although a wide range (0.05 Å) of Δr for the difference in Si-O and P-O bond lengths has been reported.^{71,88,89}

Accurate vibrational envelopes have been calculated for Si, P, As, Ge, and B molecules,^{41,42,44,87} but the calculations are much more difficult for condensed solids and have not been performed except for adsorbed CO on Ni.⁵⁶

To more fully appreciate the effects of FSVB on solid-state XPS linewidths, Δr values for the Si-O bond length in solid SiO₂ and the gas phase analog Si(OCH₃)₄ were calculated to determine the influence of three-dimensional network bonding in solid SiO₂ relative to gas phase analog Si(OCH₃)₄. The structures for α -SiO₂ and Si(OCH₃)₄ are shown in Figs. 3(a) and 3(b). The calculated ground state Si-O bond lengths are (Table III) within 0.015 Å of the experimental values for both SiO₂ (Refs. 88 and 89) and Si(OCH₃)₄,⁷⁷ and these bond lengths are virtually identical at 80 and 300 K (within 0.003 Å). The changes to bond lengths after removal of a Si 2p and O 1s electron are listed in Tables II–IV. The change in Si-O bond lengths after Si 2p ionization for both SiO₂ and Si(OCH₃)₄ is similar, and the Si-O bond lengths [Si1-O_{1,2,3,4} for SiO₂ (Table II) and Si-O_{1,2,3,4} (Table IV right column)] *decrease* by 0.04 Å in *both* compounds. The Si 2p vibrational envelopes (and overall broadening) in both gas phase and solid-state compounds are consequently expected to be similar, although the Si-O symmetric stretching frequency in SiO₂ is significantly larger than for Si(OCH₃)₄ (Table I). Our calculations yield Δr values similar to values obtained previously using other theoretical methods on Si and B gas phase molecules,^{43,44} so that our transition state method, with removal of half a Si 2p electron, gives reasonable results compared to other theoretical calculations on gas phase molecules. Note in Tables II and IV that the O-Si2 bond lengths in SiO₂ (Table II) and O-C bond lengths in Si(OCH₃)₄ *increase* on Si 2p ionization by over 0.02 Å to compensate for the above decreases in the Si-O1 and Si-O bond lengths.

The changes in O-Si bond length after O 1s ionization for both SiO₂ and Si(OCH₃)₄ are also similar, with the O-Si bond length *increasing* by 0.05–0.06 Å in *both* compounds (Tables II–IV). Again, other bond lengths decrease to compensate. As for the Si 2p vibrational envelopes, the O 1s vibrational envelopes for the two compounds should be similar. Furthermore, a larger vibrational envelope and broader overall linewidth is expected for O 1s spectra compared to Si 2p spectra because of the larger Δr on O 1s ionization. Similar $|\Delta r|$ values for the gas phase and solid-state com-

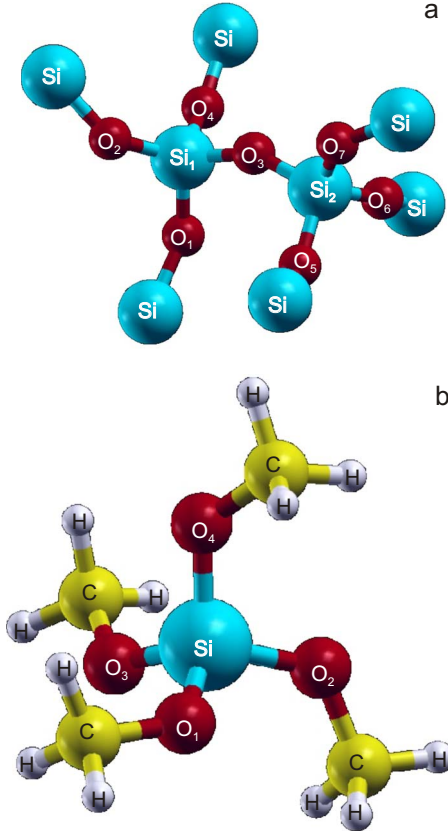


FIG. 3. (Color online) (a) Atoms and their respective labels used in the reported parameters for the α -SiO₂ simulations; (b) atoms and their respective labels used in the reported parameters for the Si(OCH₃)₄ simulations.

pounds imply that relaxation upon ionization is similar in both states of matter, and the FSVB effects in solids consequently should be similar to gas phase analogs.

C. Simulation of the Si 2*p* solid-state spectra from the gas phase Si 2*p* spectra

Completely resolved Si 2*p* spectra have been published previously for SiH₄, SiF₄, and SiCl₄,^{41,43} and vibrational structures are similar for SiF₄, SiCl₄, and Si(OCH₃)₄.^{41,55}

TABLE II. SiO₂ at 80 K: Si 2*p* ground state and HCH MD results from removal of a Si 2*p* electron (Si1*) [see Fig. 3].

Bond	Ground state (Å)	Si 2 <i>p</i> HCH (Å)	Δr (Å) ^a
Si1*-O1	1.6224	1.5846	-0.0378
Si1*-O2	1.6267	1.5888	-0.0379
Si1*-O3	1.6264	1.5890	-0.0374
Si1*-O4	1.6224	1.5845	-0.0379
O1-Si	1.6270	1.6559	0.0289
O2-Si	1.6223	1.6489	0.0266
O3-Si2	1.6219	1.6489	0.0270
O4-Si	1.6269	1.6558	0.0289

^a $\Delta r = r_{\text{HCH}} - r_{\text{ground state}}$.

TABLE III. SiO₂ at 80 K: O 1*s* ground state and HCH MD results from removal of an O 1*s* electron (O3*)⁽¹⁾ [see Fig. 3] at 80 K.

Bond	Ground state (Å)	O 1 <i>s</i> HCH (Å)	Δr (Å) ^a
Si1-O1	1.6224	1.6013	-0.0211
Si1-O2	1.6267	1.6087	-0.0180
Si1-O3*	1.6264	1.6742	0.0478
Si1-O4	1.6224	1.6036	-0.0188
O3*-Si2	1.6219	1.6649	0.0430
Si2-O5	1.6269	1.6094	-0.0175
Si2-O6	1.6267	1.6048	-0.0219
Si2-O7	1.6222	1.6061	-0.0161
O1-Si	1.6270	1.6369	0.0099
O2-Si	1.6223	1.6356	0.0133
O4-Si	1.6269	1.6403	0.0134
O5-Si	1.6224	1.6341	0.0117
O6-Si	1.6223	1.6307	0.0084
O7-Si	1.6267	1.6416	0.0149

^a $\Delta r = r_{\text{HCH}} - r_{\text{ground state}}$.

There are nine vibrational peaks for the Si 2*p*_{3/2} and Si 2*p*_{1/2} peaks of SiF₄ [Fig. 4(a)] and SiCl₄ [Fig. 4(b)] (Ref. 43) and ten for Si(OCH₃)₄ (Ref. 55) (although the number may be nine because the individual peaks were not well resolved). Both the Si 2*p*_{3/2} and Si 2*p*_{1/2} peaks are asymmetric about the most intense peak, with the vibrational intensities being more intense on the *high* binding energy side of the most intense peak [i.e., Fig. 4 where peak 2 is larger than 2' and 3 is larger than 3']. These spectra show that the symmetric stretch in the ion state ($\nu=0.111$ eV or 895 cm⁻¹ for SiF₄ and $\nu=0.058$ eV or 470 cm⁻¹ for SiCl₄) dominates both spectra. There is no indication of a contribution from another vibrational mode, which is consistent with the expected symmetric relaxation about a tetrahedral Si atom when a Si 2*p* electron is removed. This vibrational pattern will be identical

TABLE IV. Si(OCH₃)₄ at 80 K, MD results for removal of a Si 2*p* electron and an O 1*s* electron from O3 [see Fig. 3].

Bond	O 1 <i>s</i> (O3*), Δr (Å) ^a	Si 2 <i>p</i> , Δr (Å)
$\Delta(\text{Si-O1})$ (Å)	-0.0258	-0.0405
$\Delta(\text{Si-O2})$ (Å)	-0.0262	-0.0392
$\Delta(\text{Si-O3})$ (Å)	0.0583	-0.0394
$\Delta(\text{Si-O4})$ (Å)	-0.0217	-0.0416
$\Delta(\text{O1-C})$ (Å)	0.0099	0.0213
$\Delta(\text{O2-C})$ (Å)	0.0127	0.0237
$\Delta(\text{O3-C})$ (Å)	0.0206	0.0204
$\Delta(\text{O4-C})$ (Å)	0.0121	0.0207
$\Delta(\text{C-H})$ (Å)	-0.0036	-0.0039
$\Delta(\text{O-Si-O})$ (deg)	0.3	0.0
$\Delta(\text{Si-O-C})$ (deg)	2.4	0.4
$\Delta(\text{O-C-H})$ (deg)	-1.0	-1.0

^a $\Delta r = r_{\text{HCH}} - r_{\text{ground state}}$.

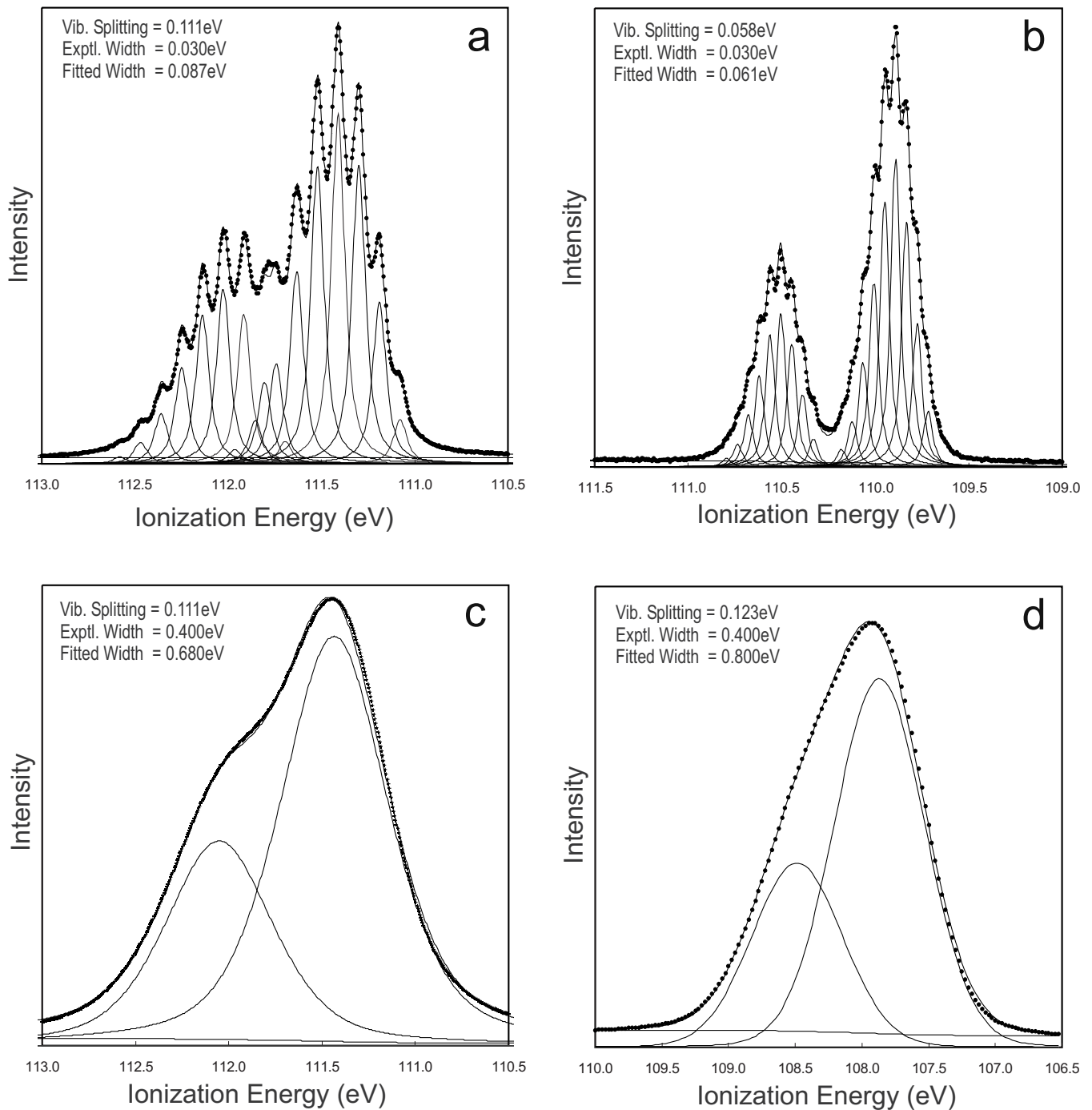


FIG. 4. The experimental high resolution Si 2*p* spectra (instrumental resolution of 30 meV) of (a) SiF₄ and (b) SiCl₄ (Ref. 43) fit to nine vibrational peaks for both the Si 2*p* spin-orbit components. Simulated spectra of SiF₄ and Si(OCH₃)₄ at our instrumental resolution of 0.4 eV are shown in (c) and (d), respectively.

at 80 and 300 K, as indicated by the virtually identical calculated changes in bond length at the two temperatures. Also, the vibrational splittings in the ion state are consistently about 10% larger than in the ground state [e.g., 895 cm⁻¹ in the ion state versus 801 cm⁻¹ in the ground state of SiF₄ (Table I)]. The SiF₄ and Si(OCH₃)₄ spectra⁵⁵ are similar, as expected by the similar Si-X (X=F, O) bond lengths and vibrational frequencies (Table I). We use these gas phase Si 2*p* spectra to simulate the Si 2*p* spectrum of solid-state SiO₂.

The spectra for SiF₄ ($\nu=895$ cm⁻¹) and Si(OCH₃)₄ ($\nu=992$ cm⁻¹) have been simulated using our experimental (lower) resolution of 0.4 eV and are shown in Figs. 4(c) and 4(d), respectively, accompanied by a fit to a Si 2*p* doublet. Changing the individual peak shapes from 85% Lorentzian (in the original spectrum) to 50% Lorentzian (because of the large expected Gaussian component from the 0.4 eV electron/photon contributions) at the lower resolution had little effect on the total Si 2*p*_{3/2} linewidths. For example, the

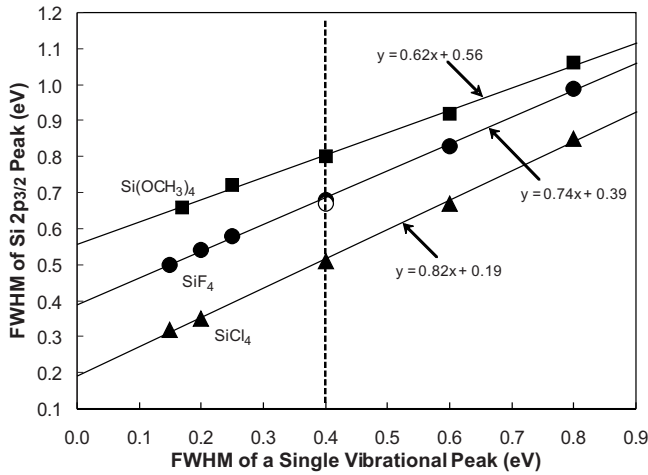


FIG. 5. The full width at half maxima (FWHM) of the Si $2p_{3/2}$ peak obtained by our spectral simulations versus the FWHM of a single vibrational peak for the three gas phase Si $2p$ spectra: from top to bottom, $\text{Si}(\text{OCH}_3)_4$, SiF_4 , and SiCl_4 . The linear relationship is indicated by the least-squares fits for all three molecules.

linewidths in Fig. 4(c) decreased by less than 0.02 eV from the 85% case to the 50% Lorentzian case. The asymmetry in the high resolution spectrum [Fig. 4(a)] is not readily observed in the two doublet fits in Figs. 4(c) and 4(d) due primarily to the Si $2p_{1/2}$ peak accommodating much of the asymmetry.

As expected, the vibrational splittings are no longer resolved in Figs. 4(c) and 4(d), and even the spin-orbit splitting is indistinct. These two spectra are qualitatively similar to the solid-state Si $2p$ spectra in Figs. 1(a)–1(c). The linewidths in the simulated spectra of 0.68 eV [Fig. 4(c)] and 0.80 eV [Fig. 4(d)] with individual peak widths of 0.4 eV (instrumental resolution) already approach the observed Si $2p_{3/2}$ total linewidths observed for the solid-state SiO_2 spectra [1.1 eV (Table I)].

Broadened Si $2p$ spectra were again simulated for all three gas phase species by varying the individual peak widths from 0.15 to 0.8 eV, and each spectrum was fit again to a spin-orbit doublet to obtain the Si $2p_{3/2}$ linewidth. The variation in Si $2p_{3/2}$ linewidths for the different individual peak widths is provided in Fig. 5 along with a linear best fit. Four observations are apparent. First, the overall linewidths vary linearly with the individual peak width (instrumental, phonon, etc.; see below) of each vibrational peak. Second, the Si $2p_{3/2}$ width increases markedly with the vibrational frequency for similar vibrational envelopes. Thus the linewidths at an individual peak width of 0.4 eV are 0.50, 0.68, and 0.80 eV for SiCl_4 , SiF_4 , and $\text{Si}(\text{OCH}_3)_4$, respectively. Third, the slopes of these lines (see equations in Fig. 5) decrease as the vibrational splitting increases from 0.82 for SiCl_4 to 0.74 for SiF_4 to 0.62 for $\text{Si}(\text{OCH}_3)_4$. Fourth, the Si $2p_{3/2}$ width approaches the individual peak width at large individual peak widths. At an individual peak width of 0.8 eV, for example, the Si $2p_{3/2}$ linewidth is 0.83 eV for SiCl_4 .

V. DISCUSSION

A. Contributions to the Si $2p$ linewidths

In the gas phase spectra [Figs. 4(a) and 4(b)], there are only two significant contributions to the Si $2p$ individual linewidths for these tetrahedral gas phase molecules: the experimental photon plus electron resolution (Γ_{ex}) and the inherent Heisenberg lifetime linewidth (Γ_{H}). The total observed linewidth (Γ_{tot}) is approximated well by^{61,90}

$$\Gamma_{\text{tot}}^2 = \Gamma_{\text{ex}}^2 + \Gamma_{\text{H}}^2. \quad (1)$$

For the SiF_4 spectrum [Fig. 4(a)], $\Gamma_{\text{tot}} = 87$ meV and $\Gamma_{\text{ex}} = 30$ meV (both observed), yielding $\Gamma_{\text{H}} = 82$ meV for each of the vibrational peaks, in close agreement with a better deconvolution method which yielded 79 meV.⁴³ This example illustrates that the 30 meV experimental width adds less than 10 meV to the total linewidth above the Heisenberg linewidth Γ_{H} . Changes in inherent Si $2p$ linewidths due to different chemical environments^{41–43} are also small. The variation in Γ_{H} for Si $2p$ ranges from 38 meV for SiH_4 to 79 meV for SiF_4 .⁴³ With our Γ_{ex} of 0.4 eV, substituting the Γ_{H} values of 38 and 79 meV gives Γ_{tot} values of less than 0.41 eV in both cases. This shows clearly that small differences in Γ_{H} make no significant difference to Γ_{tot} .

Ligand field or molecular field splitting^{45,90–92} may also split the Si $2p_{3/2}$ in nontetrahedral gas phase Si compounds. Such splitting or broadening has been observed on $2p_{3/2}$ levels of asymmetric molecules such as H_2S (Ref. 92) and PF_3 (Ref. 45) and on the d levels of a host of other noncubic molecules.^{90,91} It cannot be seen in the Si $2p_{3/2}$ spectra of tetrahedral SiX_4 molecules and will not be seen on our silicates with a tetrahedral or nearly tetrahedral SiO_4 moiety.⁹⁰

In nonconductor solids, there are six additional contributions to Si $2p_{3/2}$ linewidths. These are (1) differential charge broadening (Γ_{DC}) for nonconductors, (2) broadening or asymmetry from surface contributions (Γ_{surf}), (3) chemical shift broadening from inequivalent atoms in the crystal structure (Γ_{CS}), (4) inhomogeneous work functions from band bending variations (Γ_{WF}),^{7,48} (5) final state vibrational contributions (Γ_{FSVB}), which should be temperature independent below room temperature; and (6) phonon broadening (Γ_{PB}), which is temperature dependent.

The first four are not significant. As previously emphasized in Sec. IV, differential charge broadening (Γ_{DC}), even on rough nonconductors, is less than 0.1 eV for the XPS spectra taken with the Kratos instrument. The As $3d$ linewidths on a semiconductor (FeAsS) and a chemically similar nonconductor (As_2S_3) had identical and narrow linewidths of 0.51 eV.⁸ Many repeat spectra of the same material but from different surfaces (e.g., crystalline SiO_2) give similar linewidths and shapes. Also, the similarity of linewidths for our SiO_2 studies and for the noncharging thin film SiO_2 (Refs. 48 and 80) shows that differential charge broadening in our spectra is significantly less than 0.1 eV. Second, surface core-level shifts and unique surface electronic states of polar compounds^{49,50,93–95} (Γ_{surf}) may contribute an additional peak up to about 10% of the intensity of the main peak with Al $K\alpha$ photons. Such surface contributions on an oxide, Cu_2O , are very small²² and will not contribute significantly

(<0.1 eV) to a one-peak width. A third contribution from inequivalent structural sites in crystals (Γ_{CS}) does not apply to Si atoms in this study. In all samples studied here, the Si and other “central” atoms are in a unique position,^{67,87,88,96} even though *M*-O bond lengths are not always equivalent. There are, for example, two pairs of Si-O bond lengths of 1.607 and 1.611 Å (Refs. 89 and 96) in α -SiO₂ [about 0.015 Å smaller than our calculations (Table II)]. For Mg₂SiO₄, the Si-O bond lengths vary more than in quartz and lead to three chemically different oxygen atoms in each structure,^{88,97} but the central Si atoms are nevertheless restricted to one structural site. Thus, there can be no Si 2*p* chemical shift broadening for Si atoms in this study. The fourth contribution, inhomogeneous work functions, has been shown to shift peaks in thin film spectra up to ~0.1 eV (Ref. 48) and give measured linewidth differences of up to 0.09 eV on the Ti 2*p* level in semiconductor thin film TiO₂ samples.⁷ However, the similarity of our Si 2*p*_{3/2} linewidths for α -SiO₂ and with nonconducting thin film SiO₂ samples^{48,80} shows that this effect should give linewidth broadening of less than 0.1 eV.

There remain only two sources of the large linewidth broadening in the materials here studied (in addition to the experimental broadening of ~0.4 eV for the Kratos instrument). These are final state vibrational broadening (Γ_{FSVB}) and phonon broadening contributions (Γ_{PB})—the contributions that have been important for the adsorbed molecules and cluster species.^{63,64}

The previously discussed theoretical calculations indicate that Si 2*p* vibrational profiles should be similar in solid silicates and in gaseous Si(OCH₃)₄, so that their Si 2*p* vibrational envelopes should also be similar. Figure 5 shows that the ion state vibrational splittings greatly increase the Si 2*p*_{3/2} “total” linewidth of Si(OCH₃)₄ to approximately 0.8 eV at our experimental resolution of 0.4 eV, accounting for much of the observed total Si 2*p*_{3/2} linewidth of 1.1 eV for α -SiO₂. Because the ground state vibrational frequencies are even larger for SiO₂ than for Si(OCH₃)₄ or for Mg₂SiO₄, this 0.8 eV should represent a minimum Si 2*p*_{3/2} linewidth for SiO₂ at our experimental resolution of 0.4 eV. These arguments and observations demonstrate that Γ_{FSVB} makes a *significant contribution* to the Si 2*p* linewidths of about 0.8 eV in all Si 2*p* solid-state spectra.

There remains the problem to determine the individual (vibrational) peak widths for the spectra here collected. These widths have to be appreciably greater than 0.4 eV because of the phonon broadening contribution Γ_{PH} .

Figure 5 (and $y=0.62x+0.56$) indicates that individual peak widths (Γ_{IP} , *x* axis) are less than 0.92 and 0.84 eV for total observed Si 2*p*_{3/2} linewidths (*y* axis) of 1.13 eV ($T=300$ K) and 1.09 eV ($T=120$ K), respectively, because the vibrational splitting for SiO₂ is larger than that for Si(OCH₃)₄. To calculate the approximate phonon contribution to these ~0.8–0.9 eV individual linewidths, we remove the experimental width of 0.4 eV from Γ_{IP} using the quadratic formula in Eq. (1),

$$\Gamma_{IP}^2 = \Gamma_{ex}^2 + \Gamma_{PB}^2. \quad (2)$$

Substituting the above widths Γ_{ex} and Γ_{IP} , Γ_{PB} 's of 0.83 and 0.74 eV are obtained at 300 and 120 K, respectively. We can

then estimate the phonon linewidth $\Gamma_{PB}(0)$ ($T=0$ K) using the approximate formula,^{49,52}

$$\Gamma_{PB}^2(T_1) - \Gamma_{PB}^2(T_2) = (8/3)\Gamma_{PB}^2(0)(T_1 - T_2)/\Theta_D. \quad (3)$$

Taking the $\Theta_D=528$ K (Table I) for α -SiO₂ and substituting the above values into Eq. (3) yield

$$\Gamma_{PB}^2(0) = 1.10[\Gamma_{PB}^2(T_1) - \Gamma_{PB}^2(T_2)]. \quad (4)$$

Substituting the two linewidths, Γ_{PB} , calculated at T_1 and T_2 (with the above two Γ_{PB} values of 0.83 and 0.74 eV) yields $\Gamma_{PB}(0)=0.39$ eV. This is an approximate value (probably good to no better than 30–40 %) and is probably an upper limit because the expected Γ_{FSVB} for SiO₂ should be larger than for Si(OCH₃)₄ as mentioned above. However, these very approximate calculations indicate that the final state vibrational contributions at 300 and 120 K are similar to the phonon contributions, and the estimated Γ_{FSVB} of 0.58 eV [intercept in Fig. 5 for Si(OCH₃)₄] is larger than the estimated phonon width $\Gamma_{PH}(0)$ of 0.39 eV.

The Si 2*p*_{3/2} linewidth for Mg₂SiO₄ (0.99 eV) is substantially narrower than for SiO₂ (1.09 eV), as expected by the lower Si-O vibrational frequency in Mg₂SiO₄ compared to SiO₂. Using the Si(OCH₃)₄ line (Fig. 5), one obtains $\Gamma_{IP}=0.69$ eV and a Γ_{PB} of 0.56 eV at 300 K. Because the Si-O vibrational splittings are similar for Si(OCH₃)₄ and Mg₂SiO₄, Γ_{PB} is probably closer to the real value than the ~0.7–0.8 eV values for SiO₂ calculated above. The temperature dependence of this linewidth would now have to be obtained to yield $\Gamma_{PB}(0)$, but it is likely to be greater than that for SiO₂ because Θ_D for Mg₂SiO₄ is substantially larger than for SiO₂ (Table I). Additional low temperature studies of the linewidths for Mg₂SiO₄ are obviously required in the future.

B. Contributions to the O 1*s* linewidths

As previously emphasized, O 1*s* linewidths are appreciably larger than Si 2*p* linewidths for α -SiO₂ and other silicates. They are also asymmetric (Figs. 2 and 3). The inherent linewidth (Γ_H) for O 1*s* [0.16 eV (Ref. 56)] is larger than Si 2*p* inherent linewidths (<0.1 eV), but Γ_H is still too small to make an appreciable contribution to the increased O 1*s* width. All O atoms are equivalent in α -SiO₂,^{88,97} so there is no contribution from Γ_{CS} . The O 1*s* linewidths in silicates and in siloxane polymers³⁹ are consistently larger than the corresponding Si 2*p*_{3/2} widths indicating that the O 1*s* widths are also controlled by a large vibrational envelope. The O 1*s* vibrational envelope probably contains more than the nine peaks (as found in the Si 2*p* envelope). There are no high resolution gas phase O 1*s* data on a model compound such as Si(OCH₃)₄, so that it is not possible to estimate the number of peaks contributing to the O 1*s* envelope, the vibrational modes and splittings, or the relative intensities. For example, it is expected that the Si-O-Si bond angle of 144° in quartz⁹⁶ will yield vibrational splitting from both symmetric Si-O modes and from asymmetric modes [as seen on the O 1*s* level in H₂O (Ref. 56)].

The theoretical calculations strongly support the conclusion that the O 1*s* line in quartz should be broader than the

Si $2p_{3/2}$ line from the FSVB mechanism. There are two differences between the Si^{*}-O and O^{*}-Si bond length changes on ionization. First, the O^{*}-Si bond length increases on ionization, whereas the Si^{*}-O bond length decreases on ionization. Second, the O^{*}-Si bond length changes are larger than the Si^{*}-O bond lengths for both gas and solid compounds, indicating that there should be more vibrational peaks for O 1s spectra compared to the Si 2p spectra. Also, an increase in bond length for the O 1s ionization should lead to a larger vibrational envelope than a decrease in bond length (for the same Δr magnitude) because the slope of the low R part of the ion state potential curve is greater than the slope of the high R part of the potential curve.⁸⁶

The lack of a measurable temperature dependence on the O 1s linewidths in SiO₂ is perhaps surprising. However, Fig. 5 shows that the slope of the FWHM line decreases with an increase in vibrational frequency [e.g., from SiCl₄ to Si(OCH₃)₄], and the slope should also decrease with an increase in the number of vibrational peaks from the Si 2p spectra to the O 1s spectra. Unfortunately, without measurable temperature dependence or a better knowledge of the O 1s vibrational structure, it is not possible to estimate the phonon broadening. There is no reason to suggest, however, that $\Gamma_{\text{PH}}(0)$ is any larger for O 1s than for the Si $2p_{3/2}$ line (0.36 eV). For example, for the potassium halides,⁵¹ the anion and cation core levels have similar $\Gamma_{\text{PH}}(0)$ values.

VI. CONCLUSIONS

Our high resolution (0.4 eV instrumental resolution) Si 2p and O 1s XPS spectra of the nonconductor quartz (α -SiO₂) and vitreous SiO₂ still yield relatively broad linewidths (1 eV or greater) compared to linewidths of most semiconductors. The Si 2p linewidths are similar to that obtained on a higher resolution spectrum of a thin conducting SiO₂ film, showing that differences in inherent linewidths, chemical shift broadening, differential charging, and nonuniform work functions are not a significant cause of the large linewidths. As suggested by the core equivalent model, high quality theoretical calculations on the ground state and Si 2p and O 1s ion states of quartz (α -SiO₂) and the gas phase analog Si(OCH₃)₄ show that the bond length changes on ionization (Δr) are similar in both compounds. This suggests strongly that the Si 2p and O 1s vibrational splittings in both solid state and gas phase should be very similar. The high resolution gas phase Si 2p spectra of Si molecules, such as the analog Si(OCH₃)₄, show extensive vibrational structure and some asymmetry. Combined with the theoretical calculations, a large vibrational envelope should contribute to the Si 2p and O 1s linewidths of SiO₂. This conclusion is supported by the asymmetric linewidths of the observed O 1s peaks. Phonon broadening (PB) is shown to produce significant Si 2p line broadening, which leads to the temperature dependence of the Si 2p linewidths.

This study requires further research to confirm some of our assumptions and results. First, high resolution gas phase O 1s and metal 2p (and other central atom levels) spectra of oxygen-containing analogs such as the metal alkoxides [$M(\text{OR}_3)_4$ ($M=\text{Si}, \text{Ti}, \text{etc.}$)] need to be collected to confirm

that the O 1s vibrational envelopes yield the predicted broad (and asymmetric) O 1s lines for these compounds. Vibrational structure will not be readily resolved in the O 1s spectra because the inherent O 1s linewidth of 0.16 eV is larger than the expected vibrational splittings. However, such spectra will confirm the overall large linewidth and asymmetry of the O 1s profile and probably the nature (the importance of symmetric and asymmetric O-Si contributions) of the vibrational splitting. Second, greater effort is required to collect high resolution spectra of solids using synchrotron radiation at a range of temperatures, particularly very low temperatures. These studies need to be performed on solids with large vibrational frequencies in an attempt to resolve vibrational effects in oxides and other solids such as polymers and to determine the phonon broadening effects in these samples over a wide temperature range. Third, there needs to be a detailed study, with the same high resolution, of a number of metal oxides (mostly nonconductors) with very different M -O stretching frequencies. Our analysis predicts that the metal and O 1s linewidths (and asymmetry) should increase as the M -O frequencies increase. Already, the literature indicates that the light metal oxides such as MgO (Ref. 18) have much larger linewidths than the heavier metal oxides such as TiO₂ (Refs. 1–7) and RuO₂.^{14,15} Also, the O 1s spectra for TiO₂ show no significant asymmetry.⁵

Numerous theoretical aspects need to be addressed. Molecular dynamics calculations are required on other solids to determine the Δr values after ionization. Complete vibrational calculations on the Si 2p and O 1s vibrational profiles for solids such as SiO₂ are required. A re-examination of the phonon broadening calculations is warranted with particular emphasis on values of $\Gamma_{\text{PH}}(0)$ and the contribution of ion state profiles to these values. The $\Gamma_{\text{PH}}(0)$ values obtained by extrapolation of results in the literature typically yield rather large values for nonconductors. The large values are unexplained but may well result from final state vibrational splitting. Apart from the probable example of the Be 1s XPS of Be metal mentioned earlier,⁶² this contribution has not been included in previous theoretical treatments of core-level XPS spectra of solids.

Predictions from this study should extend the scope of nonconductor XPS studies. If there is a small M - X stretching frequency (such as in metal halides), linewidths for many compounds may approach 0.5 eV at room temperature [as observed previously for As₂S₃ (Ref. 8)]. Such linewidths (and well-behaved line shapes) are much narrower than obtained in earlier studies and should make an appreciable difference to the chemical sensitivity of XPS studies of many nonconductors. Already, McIntyre and co-workers^{23,24} have used the increased chemical sensitivity of the Kratos instrument to study multiplet effects in transition-metal oxide compounds at much better resolution than previously obtained, and we have used the increased chemical sensitivity to study leaching and the structure of silicate glasses.^{11,27,28} Second, the inherent asymmetry of the O 1s (and other peaks) must be taken into account for analysis of broad XPS spectra. A unique asymmetric O 1s peak shape needs to be agreed on to fit all the spectra of silicates and other oxides with large vibrational frequencies.

ACKNOWLEDGMENTS

We are grateful to NSERC for funding, to Surface Science Western for technical help, to T. K. Sham for a critical reading of the paper, to T. D. Thomas for very generously send-

ing us his raw Si 2*p* data for the Si 2*p* spectra of SiF₄ and SiCl₄, to A. N. Buckley and S. L. Harmer for providing us their high resolution XPS results on Cu₂O in advance of publication and also for their very helpful discussions, and to K. N. Dalby and A. R. Pratt for helpful discussions.

*Corresponding author; gmbancro@uwo.ca

- ¹H. Perron, J. Vandenborre, C. Domain, R. Drot, J. Roques, E. Simoni, J.-J. Errhardt, and H. Catalette, *Surf. Sci.* **601**, 518 (2007).
- ²P. Karmakar, G. F. Liu, and J. A. Yarmoff, *Phys. Rev. B* **76**, 193410 (2007), and references therein.
- ³G. Ketteler, S. Yamamoto, H. Bluhm, K. Andersson, D. E. Starr, D. F. Ogletree, H. Ogasawara, A. Nilson, and M. Salmeron, *J. Phys. Chem. C* **111**, 8278 (2007).
- ⁴G. J. Fleming, K. Adib, J. A. Rodriguez, M. A. Barteau, and H. Idriss, *Surf. Sci.* **601**, 5726 (2007); **602**, 2029 (2008).
- ⁵S. H. Cheung, P. Nachimuthu, A. G. Joly, M. H. Engelhard, M. K. Bowman, and S. A. Chambers, *Surf. Sci.* **601**, 1754 (2007).
- ⁶S. H. Cheung, P. Nachimuthu, M. H. Engelhard, C. M. Wang, and S. A. Chambers, *Surf. Sci.* **602**, 133 (2008).
- ⁷S. A. Chambers, T. Ohsawa, C. M. Wang, I. Lyubinetsky, and J. E. Jaffe, *Surf. Sci.* **603**, 771 (2009).
- ⁸H. W. Nesbitt, G. M. Bancroft, R. Davidson, N. S. McIntyre, and A. R. Pratt, *Am. Mineral.* **89**, 878 (2004).
- ⁹V. P. Zakaznova-Herzog, H. W. Nesbitt, G. M. Bancroft, J. S. Tse, X. Gao, and W. Skinner, *Phys. Rev. B* **72**, 205113 (2005).
- ¹⁰V. P. Zakaznova-Herzog, H. W. Nesbitt, G. M. Bancroft, and J. S. Tse, *Surf. Sci.* **600**, 3175 (2006).
- ¹¹V. P. Zakaznova-Herzog, H. W. Nesbitt, G. M. Bancroft, and J. S. Tse, *Geochim. Cosmochim. Acta* **72**, 69 (2008).
- ¹²H. J. Song, H. J. Shin, Y. Chung, J. C. Lee, and M. K. Lee, *J. Appl. Phys.* **97**, 113711 (2005), and references therein.
- ¹³Y. K. Kim, J. R. Ahn, W. H. Choi, H. S. Lee, and H. W. Yeom, *Phys. Rev. B* **68**, 075323 (2003).
- ¹⁴M. Knapp, D. Crihan, A. P. Seitsonen, E. Lundgren, A. Resta, J. N. Andersen, and H. Over, *J. Phys. Chem. C* **111**, 5363 (2007).
- ¹⁵H. Over, A. P. Seitsonen, E. Lundgren, M. Wiklund, and J. N. Andersen, *Chem. Phys. Lett.* **342**, 467 (2001).
- ¹⁶S. Altieri, S. F. Contri, and S. Valeri, *Phys. Rev. B* **76**, 205413 (2007), and references therein.
- ¹⁷V. K. Lazarov, R. Plass, H.-C. Poon, D. K. Saldin, M. Weinert, S. A. Chambers, and M. Gajdardziska-Josifovska, *Phys. Rev. B* **71**, 115434 (2005).
- ¹⁸P. Liu, T. Kendelewicz, G. E. Brown, and G. A. Parks, *Surf. Sci.* **412-413**, 287 (1998); P. Liu, T. Kendelewicz, and G. E. Brown, *ibid.* **412-413**, 315 (1998).
- ¹⁹P. Liu, T. Kendelewicz, G. E. Brown, G. A. Parks, and P. Pianetta, *Surf. Sci.* **416**, 326 (1998).
- ²⁰H.-B. Fan, S.-Y. Yang, P.-F. Zhang, H.-Y. Wei, X.-L. Liu, C.-M. Jiao, Q.-S. Zhu, Y.-H. Chen, and Z.-G. Wang, *Chin. Phys. Lett.* **24**, 2108 (2007).
- ²¹T. Kendelewicz, P. Liu, C. S. Doyle, G. E. Brown, Jr., E. L. Nelson, and S. A. Chambers, *Surf. Sci.* **453**, 32 (2000), and references therein.
- ²²S. L. Harmer, W. M. Skinner, A. N. Buckley, and L.-J. Fan, *Surf. Sci.* **603**, 537 (2009).
- ²³B. P. Payne, A. P. Grosvenor, M. C. Biesinger, B. A. Kobe, and N. S. McIntyre, *Surf. Interface Anal.* **39**, 582 (2007).
- ²⁴M. C. Biesinger, C. Brown, J. R. Mycroft, R. D. Davidson, and N. S. McIntyre, *Surf. Interface Anal.* **36**, 1550 (2004).
- ²⁵D. E. Starr, F. M. T. Mendes, J. Middeke, R.-P. Blum, H. Niehus, D. Lahav, S. Guimond, A. Uhl, T. Kluener, M. Schmal, H. Kuhlbeck, S. Shaikhutdinov, and H.-J. Freund, *Surf. Sci.* **599**, 14 (2005).
- ²⁶M. Salmeron and R. Schlogl, *Surf. Sci. Rep.* **63**, 169 (2008).
- ²⁷K. N. Dalby, H. W. Nesbitt, V. P. Zakaznova-Herzog, and P. A. King, *Geochim. Cosmochim. Acta* **71**, 4297 (2007), and references therein.
- ²⁸H. W. Nesbitt and K. N. Dalby, *Can. J. Chem.* **85**, 782 (2007).
- ²⁹D. Ehre, H. Cohen, V. Lyahovitskaya, and I. Lubomirsky, *Phys. Rev. B* **77**, 184106 (2008).
- ³⁰M. T. Rinke, L. Zhang, and H. Eckert, *ChemPhysChem* **8**, 1988 (2007).
- ³¹M. Gazda and A. Winiarski, *Physica C* **432**, 35 (2005).
- ³²M. Qvarford, S. Soderholm, G. Chiaia, R. Nyholm, J. N. Andersen, I. Lindau, U. O. Karlsson, L. Leonyuk, A. Nilsson, and N. Martensson, *Phys. Rev. B* **53**, R14753 (1996).
- ³³A. Koitzsch, J. Fink, M. S. Golden, K. Karlsson, O. Jepsen, O. Gunnarsson, L. L. Miller, H. Eisaki, S. Uchida, G. Yang, and S. Abell, *Phys. Rev. B* **66**, 024519 (2002).
- ³⁴V. R. Mastelaro, P. N. Lisboa-Filho, P. P. Neves, W. H. Schreiner, P. A. P. Nascente, and J. A. Eiras, *J. Electron Spectrosc. Relat. Phenom.* **156-158**, 476 (2007).
- ³⁵L. Lv, F. Y. Lee, J. Zhou, F. Su, and X. S. Zhao, *Microporous Mesoporous Mater.* **96**, 270 (2006).
- ³⁶R. Heuberger, A. Rossi, and N. D. Spencer, *Tribol. Lett.* **28**, 209 (2007).
- ³⁷J. B. Gustafsson, H. M. Zhang, E. Moons, and L. S. O. Johansson, *Phys. Rev. B* **75**, 155413 (2007).
- ³⁸D. L. Legrand, G. M. Bancroft, and H. W. Nesbitt, *Am. Mineral.* **90**, 1042 (2005).
- ³⁹L.-A. O'Hare, A. Hynes, and M. R. Alexander, *Surf. Interface Anal.* **39**, 926 (2007).
- ⁴⁰R. Eguchi, M. Taguchi, M. Matsunami, K. Horiba, K. Yamamoto, Y. Ishida, A. Chainani, Y. Takata, M. Yabashi, D. Miwa, Y. Nishino, K. Tamasaku, T. Ishikawa, Y. Senba, H. Ohashi, Y. Muraoka, Z. Hiroi, and S. Shin, *Phys. Rev. B* **78**, 075115 (2008).
- ⁴¹J. D. Bozek, G. M. Bancroft, J. N. Cutler, and K. H. Tan, *Phys. Rev. Lett.* **65**, 2757 (1990).
- ⁴²T. D. Thomas, L. J. Saethre, K. J. Borve, J. D. Bozek, M. Huttala, and E. Kukkk, *J. Phys. Chem. A* **108**, 4983 (2004), and references therein.
- ⁴³T. D. Thomas, C. Miron, K. Wiesner, P. Morin, T. X. Carroll, and L. J. Saethre, *Phys. Rev. Lett.* **89**, 223001 (2002).
- ⁴⁴T. D. Thomas, R. Puttner, H. Fukuzawa, G. Prumper, K. Ueda, E. Kukkk, R. Sankari, J. Harries, Y. Tamenori, T. Tanaka, M.

- Hoshino, and H. Tanaka, *J. Chem. Phys.* **127**, 244309 (2007).
- ⁴⁵K. J. Borve, L. F. Saethre, J. D. Bozek, J. True, and T. D. Thomas, *J. Chem. Phys.* **111**, 4472 (1999).
- ⁴⁶C. J. Karlsson, F. Owman, E. Landemark, Y.-C. Chao, P. Martensson, and R. I. G. Uhrberg, *Phys. Rev. Lett.* **72**, 4145 (1994).
- ⁴⁷S. M. Scholz and K. Jacobi, *Phys. Rev. B* **52**, 5795 (1995).
- ⁴⁸F. J. Himpsel, F. R. McFeely, A. Taleb-Ibrahimi, J. A. Yarmoff, and G. Hollinger, *Phys. Rev. B* **38**, 6084 (1988); F. J. Himpsel, B. S. Meyerson, F. R. McFeely, J. F. Morar, A. Taleb-Ibrahimi, and J. A. Yarmoff, in *Proceedings of the Enrico Fermi School on Photoemission and Absorption Spectroscopy of Solids and Interfaces using Synchrotron Radiation*, edited by M. Campagna and R. Rosei (North-Holland, Amsterdam, 1990), Vol. 203.
- ⁴⁹J. A. Leiro, K. Laajalehto, I. Kartio, and M. Heinonen, *Surf. Sci.* **412-413**, L918 (1998).
- ⁵⁰A. G. Schauffuss, H. W. Nesbitt, M. J. Scaini, H. Hoehst, G. M. Bancroft, and R. Szargan, *Am. Mineral.* **85**, 1754 (2000).
- ⁵¹P. R. Citrin, P. Eisenberger, and D. R. Hamann, *Phys. Rev. Lett.* **33**, 965 (1974).
- ⁵²G. D. Mahan, *Phys. Rev. B* **21**, 4791 (1980).
- ⁵³G. K. Wertheim, D. M. Riffe, and P. H. Citrin, *Phys. Rev. B* **49**, 2277 (1994).
- ⁵⁴K. Siegbahn, *J. Electron Spectrosc. Relat. Phenom.* **5**, 3 (1974); U. Gelius, *ibid.* **5**, 985 (1974).
- ⁵⁵D. G. J. Sutherland, G. M. Bancroft, and K. H. Tan, *J. Chem. Phys.* **97**, 7918 (1992), and references therein.
- ⁵⁶R. Sankari, M. Ehra, H. Nakatsuji, Y. Senba, K. Hosokawa, H. Yoshida, A. De Fanis, Y. Tamenori, S. Aksela, and K. Ueda, *Chem. Phys. Lett.* **380**, 647 (2003).
- ⁵⁷N. Martensson and A. Nilson, *J. Electron Spectrosc. Relat. Phenom.* **52**, 1 (1990), and references therein.
- ⁵⁸J. N. Andersen, A. Beutler, S. L. Sorenson, R. Nyholm, B. Setlik, and D. Heskett, *Chem. Phys. Lett.* **269**, 371 (1997).
- ⁵⁹A. Fohllisch, N. Wassdahl, J. Hasselstrom, O. Karis, D. Menzel, N. Martensson, and A. Nilsson, *Phys. Rev. Lett.* **81**, 1730 (1998).
- ⁶⁰H.-P. Steinruck, T. Fuhrmann, C. Papp, B. Trankenschuh, and R. Denecke, *J. Chem. Phys.* **125**, 204706 (2006).
- ⁶¹H. Bergersen, M. Abu-samaha, A. Lindblad, R. R. T. Marinho, D. Ceolin, G. Ohrwall, L. J. Saethre, M. Tchapyguine, K. J. Borve, S. Svensson, and O. Bjorneholm, *Chem. Phys. Lett.* **429**, 109 (2006).
- ⁶²J. N. Andersen, T. Balasubramanian, C.-O. Almbladh, L. I. Johansson, and R. Nyholm, *Phys. Rev. Lett.* **86**, 4398 (2001).
- ⁶³P. J. Feibelman, *Phys. Rev. B* **49**, 13809 (1994).
- ⁶⁴N. V. Dobrodey, A. I. Streltsov, and L. S. Cederbaum, *Phys. Rev. A* **65**, 022501 (2002).
- ⁶⁵Kratos web page: <http://www.kratos.com>
- ⁶⁶D. A. Shirley, *Phys. Rev. B* **5**, 4709 (1972).
- ⁶⁷Neal Fairley, CASAXPS, Version 2.1.26, 1999, <http://www.casaxps.com>
- ⁶⁸CPMD (1990–2004), Copyright IBM Corp., MPI für Festkörperforschung Stuttgart, 1997.
- ⁶⁹J. P. Perdew, K. Burke, and M. Ernzerhof, *Phys. Rev. Lett.* **77**, 3865 (1996).
- ⁷⁰N. Troullier and J. L. Martins, *Phys. Rev. B* **43**, 1993 (1991).
- ⁷¹S. V. Churakov, N. R. Kishina, V. S. Urusov, and R. Wirth, *Phys. Chem. Miner.* **30**, 1 (2003).
- ⁷²D. M. Shaw and J. S. Tse, *Am. Mineral.* **92**, 1593 (2007).
- ⁷³J. C. Slater, *The Self-Consistent Field for Molecules and Solids, Quantum Theory of Molecules and Solids* (McGraw-Hill, New York, 1974), Vol. 4.
- ⁷⁴S.-D. Mo and W. Y. Ching, *Appl. Phys. Lett.* **78**, 3809 (2001).
- ⁷⁵R. T. Downs and M. Hall-Wallace, *Am. Mineral.* **88**, 247 (2003).
- ⁷⁶R. M. Hazen, L. W. Finger, R. J. Hemley, and H. K. Mao, *Solid State Commun.* **72**, 507 (1989).
- ⁷⁷L. H. Boonstra, F. C. Mijlhoff, G. Renes, A. Spelbos, and I. Hargittai, *J. Mol. Struct.* **28**, 129 (1975).
- ⁷⁸G. Schaftenaar and J. H. Noordik, *J. Comput.-Aided Mol. Des.* **14**, 123 (2000).
- ⁷⁹M. J. Frisch *et al.*, GAUSSIAN 03, Revision C.02, Gaussian, Inc., Wallingford CT, 2004.
- ⁸⁰M. D. Ulrich, J. G. Hong, J. E. Rowe, G. Lucovsky, A. S.-Y. Chan, and T. E. Madey, *J. Vac. Sci. Technol. B* **21**, 1777 (2003).
- ⁸¹A. Shchukarev, J. Rosenqvist, and S. Sjöberg, *J. Electron Spectrosc. Relat. Phenom.* **137-140**, 171 (2004).
- ⁸²V. C. Farmer, *The Infrared Spectra of Minerals* (Mineralogical Society, London, England, 1974).
- ⁸³K. N. Dalby and P. L. King, *Am. Mineral.* **91**, 1783 (2006).
- ⁸⁴T. X. Carroll, N. Berrah, J. D. Bozek, J. Hahne, E. Kukk, L. J. Saethre, and T. D. Thomas, *Phys. Rev. A* **59**, 3386 (1999).
- ⁸⁵R. W. Shaw and T. D. Thomas, *Chem. Phys. Lett.* **22**, 127 (1973).
- ⁸⁶D. J. Bristow and G. M. Bancroft, *J. Am. Chem. Soc.* **105**, 5634 (1983).
- ⁸⁷Z. F. Liu, G. M. Bancroft, J. N. Cutler, D. G. J. Sutherland, K. H. Tan, J. S. Tse, and R. G. Cavell, *Phys. Rev. A* **46**, 1688 (1992).
- ⁸⁸W. A. Deer, R. A. Howie, and J. Zussman, *Rock-Forming Minerals—Orthosilicates*, 2nd ed. (Longmans, London, 1982), Vol. 1A.
- ⁸⁹W. A. Deer, R. A. Howie, W. S. Wise, and J. Zussman, *Rock-Forming Minerals—Framework Silicates*, 2nd ed. (Geological Society, London, 2004), Vol. 4B.
- ⁹⁰G. M. Bancroft and Y. F. Hu, in *Inorganic Electronic Structure and Spectroscopy*, edited by A. B. P. Lever and E. I. Solomon (Wiley, New York, 1999), Vol. 1, p. 443.
- ⁹¹J. N. Cutler, G. M. Bancroft, D. G. Sutherland, and K. H. Tan, *Phys. Rev. Lett.* **67**, 1531 (1991).
- ⁹²S. Svensson, A. Ausmees, S. J. Osborne, G. Bray, F. Gel'mukhanov, H. Agren, A. Naves de Brito, O.-P. Sairanen, A. Kivimaki, E. Nommiste, H. Aksela, and S. Aksela, *Phys. Rev. Lett.* **72**, 3021 (1994).
- ⁹³S. Hufner, *Photoelectron Spectroscopy: Principles and Applications*, Springer Series in Solid State Physics (Springer Verlag, Berlin, 1995), Chap. 8.
- ⁹⁴H. W. Nesbitt and I. J. Muir, *Geochim. Cosmochim. Acta* **58**, 4667 (1994).
- ⁹⁵M. F. Hochella and A. H. Carim, *Surf. Sci.* **197**, L260 (1988).
- ⁹⁶Y. Lepage and G. Donnay, *Acta Crystallogr., Sect. B: Struct. Crystallogr. Cryst. Chem.* **32**, 2456 (1976).
- ⁹⁷K. Ishii, *Am. Mineral.* **63**, 1198 (1978), and references therein.
- ⁹⁸J. A. Gadsen, *Infrared Spectra of Minerals and Related Compounds* (Butterworths, London, England, 1975).
- ⁹⁹W. Kieffer, Ph.D. thesis, California Institute of Technology, 1971.
- ¹⁰⁰R. A. Robie and J. L. Edwards, *J. Appl. Phys.* **37**, 2659 (1966).
- ¹⁰¹K. Nakamoto, *Infrared Spectra of Inorganic and Coordination Compounds*, 4th ed. (Wiley-Interscience, New York, 1986); *Infrared Spectra of Inorganic and Coordination Compounds*, 2nd ed. (Wiley-Interscience, New York, 1970).